JOURNAL OF NEUROTRAUMA
Volume 22, Number 10, 2005

Pp. 1092–1111

Intravenous Polyethylene Glycol Inhibits the Loss of Cerebral Cells after Brain Injury

ANDREW O. KOOB,[1] BRADLEY S. DUERSTOCK,[2] CHARLES F. BABBS,[2] YINLONG SUN,[3] and RICHARD B. BORGENS[2,4]

ABSTRACT

We have tested the effectiveness of polyethylene glycol (PEG) to restore the integrity of neuronal membranes after mechanical damage secondary to severe traumatic brain injury (TBI) produced by a standardized head injury model in rats. We provide additional detail on the standardization of this model, particularly the use and storage of foam bedding that serves to both support the animal during the impact procedure—and as a dampener to the acceleration of the brass weight. Further, we employed a dye exclusion technique using ethidium bromide (EB; quantitative evaluation) and horseradish peroxidase (HRP; qualitative evaluation). Both have been successfully used previously to evaluate neural injury in the spinal cord since they enter cells when their plasma membranes are damaged. We quantified EB labeling (90 μM in 110 μL of sterile saline) after injection into the left lateral ventricle of the rat brain 2 h after injury. At six h after injection and 8 h after injury, the animals were sacrificed and the brains were analyzed. In the injured rat brain, EB entered cells lining and medial to the ventricles, particularly the axons of the corpus callosum. There was minimal EB labeling in uninjured control brains, limited to cells lining the luminal surfaces of the ventricles. Intravenous injections of PEG (1 cc of saline, 30% by volume, 2000 MW) immediately after severe TBI resulted in significantly decreased EB uptake compared with injured control animals. A similar result was achieved using the larger marker, HRP. PEG-treated brains closely resembled those of uninjured animals.

Key words: brain injury; degeneration; ethidium bromide; neuroprotection; polyethylene glycol (PEG)

INTRODUCTION

In the United States, the leading cause of death and disability for children and adults is traumatic brain injury (TBI). One and a half million Americans are injured each year; 230,000 of these people are hospitalized, but survive their injury, while 50,000 die. Approximately 80,000–90,000 sustain disabilities that affect them over a long period of time, indeed often the rest of their lives (Thurman et al., 1999). Currently, pharmacological treat-

[1]Center for Paralysis Research, Department of Biological Sciences, Program in Neuroscience, Purdue University, West Lafayette, Indiana.
[2]Center for Paralysis Research, Department of Basic Medical Sciences, Purdue University, West Lafayette, Indiana.
[3]Department of Computer Sciences, Purdue University, West Lafayette, Indiana.
[4]Department of Biomedical Engineering, College of Engineering, Purdue University, West Lafayette, Indiana.

ments are not available to these patients that have been shown to produce substantial benefits (Vink et al., 2001).

Mechanical damage to cell membranes associated with TBI is believed to progress from an initial ionic derangement when the permeability barrier provided by the plasmalemma is breached (Borgens, 1988; Povlishock et al., 1997). This may eventually produce necrotic or apoptotic cell death (Shapira et al., 1989; Gwag et al., 1999; Zipfel et al., 2000). This progressive loss of parenchyma is often referred to as "secondary injury" and may occur for many hours to days post-injury (Borgens, 2003). The most immediate—and clinically relevant—consequence, however, is the loss in neuronal excitability producing initial and progressive functional losses (Borgens, 2003). Many different pharmacological approaches that vitiate the pathological responses to TBI have been developed and tested (Keane, 2001; Vink et al., 2001). In experimental animals, promising avenues include the use of serine protease inhibitors (Movsesyan et al., 2001), caspase and calpain inhibitors (Buki et al., 2004; Feng et al., 2003), and mild, post-traumatic hypothermia (Koizumi and Povlishock, 1998). However, the injury pathway associated with mechanical trauma to cells involves many factors (Roy and Sapolsky, 1999; Raghupathi et al., 2000; Borgens, 2003), and there are still significant theoretical and practical hurdles in applying this knowledge to the development of clinical therapies for severe head injury.

Several families of inorganic hydrophilic polymers [poloxamers, poloxamines, polyethylene glycol (PEG)] are able to immediately reconstitute cell membrane damaged by mechanical injury (Borgens, 2003). PEG is a non-toxic substance that can be injected into the bloodstream and has been shown to both fuse and/or repair damaged cell membranes to stave the potential for ion influx and the resulting cell death cascade (Borgens, 2001). Topical application to isolated and injured guinea pig spinal cord white matter *in vitro*—or topical or intravenous application of PEG *in vivo*—can reverse physiological conduction block, and dramatically increase the number of surviving axons and thus the overall amount of spared white matter. This is associated with a rapid physiological and/or functional recovery in mammals (Borgens 2001, 2003). PEG has also been shown to inhibit free radical production (Luo et al., 2002) and reduce oxidative stress resulting from spinal cord injury (Luo et al., 2004).

Here, for the first time, we test the effectiveness of intravenous PEG administration in adult rats as a prophylactic to advancing cell disruption and death after traumatic TBI. To evaluate PEG's effect on cell damage, ethidium bromide (EB) was injected into the ventricular space two hours after injury and allowed to diffuse into brain tissue for six hours. EB has been used previously to detect neural injury in the spinal cord (Luo et al., 2002) because it selectively labels cells when their plasma membrane is compromised (Aeschbacher et al., 1986; Luo et al., 2002). When this fluorochrome moves unobstructed into the cytoplasmic compartment, its fluorescent intensity increases 40-fold after binding to nucleic acids, which also inhibits back-diffusion (Aeschbacher et al., 1986; Dey and Majumder, 1988; Sun-Kyung and Hollenbeck,1995 ; Koenig and Giuditta, 1999; Luo et al, 2002; Piper and Holt, 2004). Our results indicate intravenous treatment with PEG substantially prevents the uptake of this label into cerebral cells after TBI, further confirmed by a marked reduction in HRP uptake by the cells of damaged, but PEG- treated, brains.

MATERIALS AND METHODS

Impact Acceleration Injury Model

The impact acceleration brain injury device (Marmarou et al., 1994) (Fig. 1) produces injury to cells within the brain. Typical regions of the brain are particularly vulnerable after impact, including cells and processes within the corpus callosum, corona radiata, and brain stem, as well as subarachnoid hemorrhage in severe cases within the forebrain and hindbrain (Foda and Marmarou, 1994). Further descriptive and methodological details of this model can be found elsewhere (Nawashiro, 1995; Nawashiro et al., 1995; Povlishock et al., 1997.

A total of 20 rats were used in this study. For the quantitative evaluation of EB labeling, three groups of four animals weighing 400–450 g were initially anesthetized with 4% isoflurane in 99% oxygen. They were endotracheally intubated and ventilated with 1.5–2.5% isoflurane in 99% oxygen on a Harvard Apparatus Small Animal Volume Controlled Ventilator (model 683). Body temperature was maintained with a Harvard Apparatus Homeothermic Blanket Control Unit (catalog no. BS4 50-7053-R). A superficial midline incision to the scalp was performed, after which the periosteal membranes were removed to expose the skull. A metal disk (referred to below as a "helmet"), 10 mm in diameter and 3 mm wide, was firmly attached to the exposed bone with dental acrylic and Loctite QuickTite super glue gel between lambda and bregma sutures (Fig. 1). With one exception, a 450-g brass weight was dropped from a height of 2 m through a Plexiglas delivery tube onto the disc to produce a severe injury. The exception was qualitative data derived from Hemotoxylin and Eosin staining, which was performed early in these investigations after a 1.5-m drop. Immediately after the injury, a 1-cc intravenous injection of sterile saline or PEG-saline solution (2000 MW, 30% by volume) was administered into the lateral tail vein.

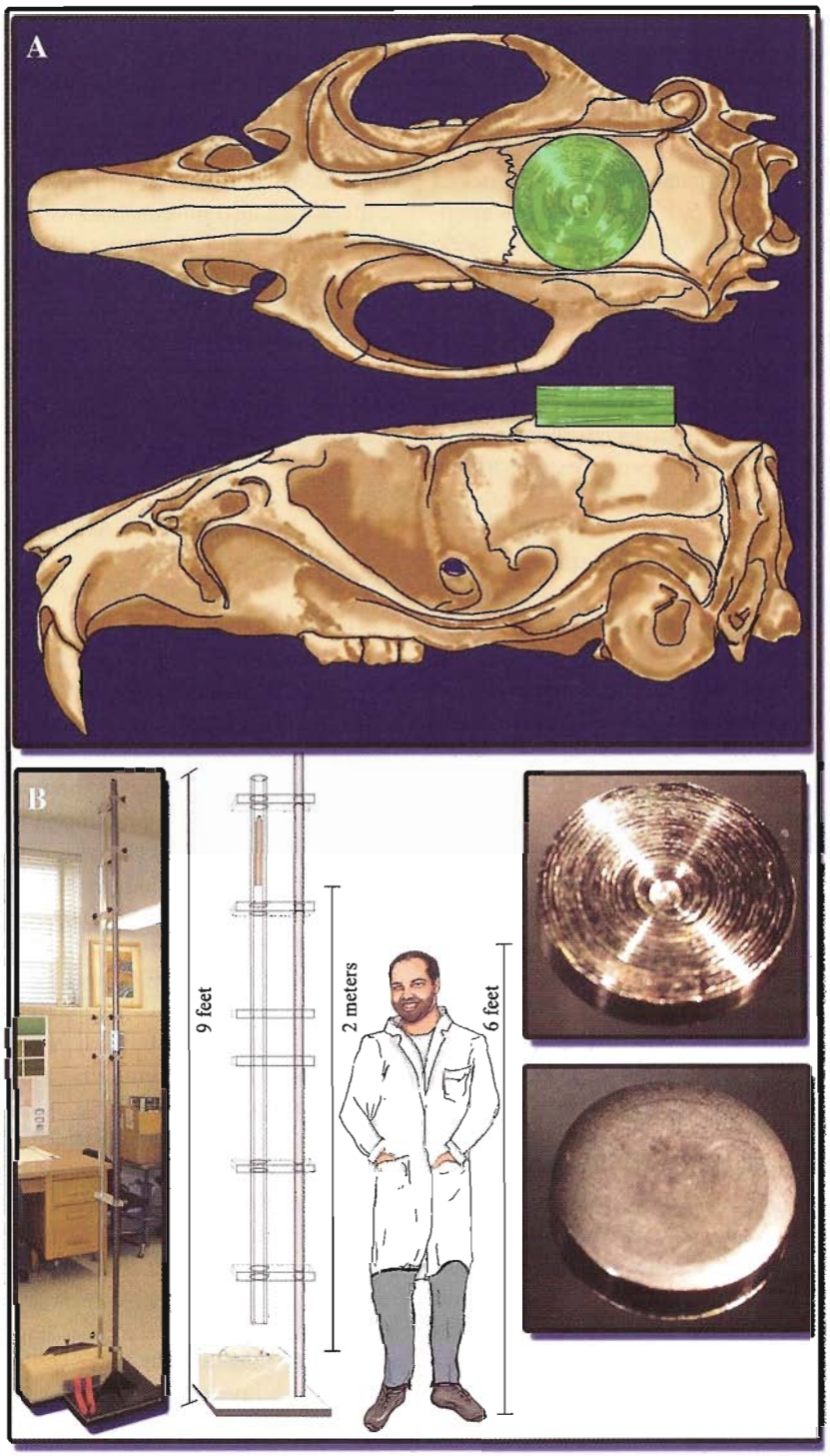

FIG. 1. Impact acceleration model. (**A**) Dorsal (top) and lateral (bottom) view of rat skull. The position of the metal helmet (green) is shown placed between the bregma suture (rostral) and the lambda suture (caudal). (**B**) From left to right: The photograph shows the impact acceleration device, whereas the adjacent diagram provides further detail; a brass weight (18 mm diameter, 7 in long, 450 g) was dropped from varying heights to provide different degrees of injury. The rat was positioned on a foam bed as shown; the insets provide detail of the helmet. A ventral view (top) of the helmet shows the concentric grooves, which provide purchase against the skull, and the smooth dorsal surface of the helmet where impact occurs (bottom).

Uninjured control animals received identical surgical and anesthetic methods, but without TBI (a weight was dropped near but not on the animal, referred to below as "sham" injury or "controls") or an injection of saline or PEG. After injury, animals were also injected intramuscularly with 0.075 mg/kg of buprenorphine HCl, allowed 15–20 min on 1.5% isoflurane in 99% oxygen. Afterwards, they were ventilated for 10 min on 99% oxygen alone and 10 min on room air. Then the animals were checked periodically and taken off the ventilator when they were able to breathe on their own. All of these procedures were both formally reviewed and approved by the Purdue University Animal Care and Use committee.

Injury Standardization: Foam Rebound Measurements

Measurements of displacement and rebound of the brass weight (18 mm diameter, 7 in long, 450 g) directly onto the foam substrate (12 cm high, 43 cm long, 13 cm wide) that supports the rat during injury were made using a standard metric ruler by straightforward means. The foam tested was newly purchased foam (Foam to Size, Ashland, VA, type E bed) and old foam (exposed to light and 6 months old after purchase—same vendor). The weight was dropped from 2 m and the maximum impact into the foam was measured as well as the maximum height of the rebound of the weight. The spring constant and damping constant of the foam were determined from these measurements. The two types of foam were compared to data provided for foam bedding in Marmarou et al., 1994 using the equation of motion based upon Newton's second law, $A\ (d^2x/dt^2) + B\ (dx/dt) + Cx = D$, where A = mass = 0.45 kg; $B = \mu$ = 20.4 N-sec/m; C = k (spring constant of the foam) = 2500 Nt/m; and D = constant = mass * gravity = 4.41 Newtons. The acceleration and time of weight impact in the foam was calculated in relation to the Head Injury Criteria (HIC = $a^{-2.5} * \Delta t$, where a is the mean acceleration during impact and Δt is the duration of the impact) (Versace, 1971; Margulies and Thibault, 1992) for further comparison (Table 1). For these calculations the acceleration and contact time for the 450-g weight alone were assumed to be similar to those for the 450-g weight plus the mass of a rat's head.

Dye Exclusion Test

Two hours post injury or sham injury in each animal a small hole was drilled into the skull (1.4 mm left of midline; 0.5 mm caudal to bregma) (Singleton and Povlishock, 2004), and an injection of EB (400 MW, 90 μM EB in 110 μL of saline) was performed with a 23-gauge needle 4 mm deep into the brain into the left lateral ventricle (Fig. 2). This procedure was facilitated using a KOPF model 900 small animal stereotaxic device. The EB was slowly injected into the ventricle for approximately 30 min. Subsequently, the needle was allowed to remain in place for another 10 min before removal. This procedure eliminated the propensity for accidental aspiration of the remaining and local substance when the needle was withdrawn. At 6 h after the intraventricular injection of EB and 8 h after injury, rats were anesthetized with 1 cc sodium pentobarbital (160 mg/kg) underwent intracardiac perfusion with lactated Ringer's solution (60% NaCl, 31% $C_3H_5NaO_3$ [anhydrous], 0.3% KCl, 0.2% $CaCl_2$ [dihydrate] by volume in distilled H_2O) followed by 4% paraformaldehyde, 1% glutaraldehyde in phosphate buffered saline solution (PBS; normal saline buffered with 0.02 M NaH_2PO_4; 0.1 M Na_2HPO_4; pH 7.4). The brains were then removed and placed in PBS overnight. The cerebellum and brain stem were discarded after dissection and coronal frozen sections at 40 ìm were taken posterior (caudal) to EB injection site. Histological sections were adhered to slides, dehydrated through water, 70% alcohol, 90% alcohol, and 100% alcohol (2 min each). They were then placed in xylene for 1 h and cover-slipped with DPX mounting medium.

Sections were observed with an Olympus BX-61 fluorescent microscope (excitation filter, BP 545 nm; barrier filter, 0–590 nm; Olympus America Inc., Melville, NY), and EB fluorescent images of complete coronal sections were photographed using a 4× objective and a high-resolution CCD camera (Olympus CC12). Since the histological sections were large, the sample could not be completely captured within a single field of view. Twenty images at this magnification were required to produce a montage using MicroSuite software (Soft Imaging System, Lakewood, CO) automated with a Ludl motorized

Table 1. Calculations of Brass Weight while in Contact with Foam

Foam	*Percent of HIC (1000) ($a^{2.5}*\Delta t$) in g*	*a (m/sec^2)*	*Δt (sec)*
Marmarou	11.8%	−252.6	0.035
New	10.6%	−239.7	0.034
Aged	5.8%	−170.2	0.046

Calculating the weight rebound in relation to the Head Injury Criteria (HIC), we found foam when new was within 10–15% of Marmarou's measurements (HIC [in g] = $a^{-2.5}*\Delta$ t). Note that the average acceleration of the brass weight while in contact with the foam was also greater for newly purchased foam compared with aged foam. The aged foam dampened the weight, resulting in a longer time of contact, slowing the impact, and lessening the severity of the injury.

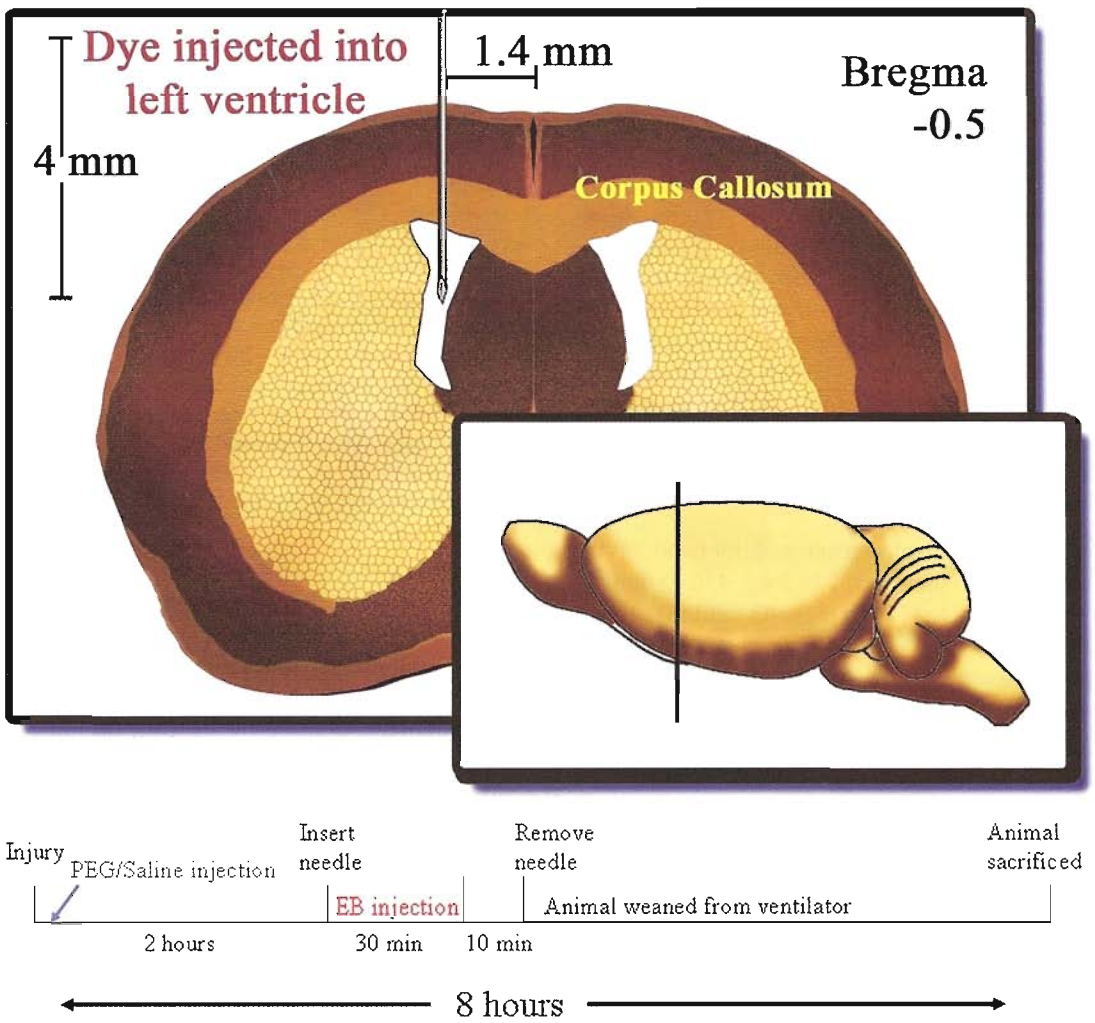

FIG. 2. Experimental procedure. (**A**) Drawing of the rat brain in coronal section. The inset shows the approximate plane of section, 0.5 mm caudal to bregma. Note the position of a 23-gauge hypodermic needle used to deliver intracellular markers into the left lateral ventricle. The anesthetized animal's head is held in place in a stereotaxic frame to facilitate the injection. Below the drawings, the experimental timeline of 8 h is depicted. The injection of PEG or control solution is made within 15 min after injury (followed by a marker dye injection approximately 2 h post-injury). This latter procedure takes 30 min. A delay of 10 min was used prior to removal of the needle. (This delay permits sufficient diffusion of the marker from its source. If the delay is not used, then some of the marker may be aspirated into the needle tract when it is withdrawn.)

stage. The completed montage provided a complete view of the histological section. Exposure settings were held constant during the capture of all digital images. Using a full coronal montage, an area between the lateral and third ventricles in a region within 1–2 mm posterior to the site of EB injection was circumscribed. Montages were obtained from this area from each animal. The acquisition and analysis of the fluorescent intensity data inside the sample area was completed using an image analysis program, Sigmascan Pro (SPSS Science, Chicago, IL) and adjusted for background fluorescence. The mean fluorescent intensity of the three sections for each animal was calculated. Units of luminosity (LUM) was determined from pixel values, and in the software used, ranged from 0 (black) to 256 (white) (Luo et al., 2003; Teng et al., 2004). All photomicrographs were taken at the same exposure, and in each montage, the mean luminosity of the lateral cortex contralateral to the injection site was subtracted from the mean luminosity of the region of interest to eliminate background fluorescence between sections (i.b.i.d.). These procedures were carried out on coded samples by personnel unaware of the experimental status of the animals provided them. The means for four animals in each group were averaged and statisti-

cally analyzed between groups with one-way ANOVA and Student-Newman-Keuls multiple comparisons tests. Significance was established with p values of ≤ 0.05.

Three-Dimensional Visualization

Acquisition of serial images. Transverse fluorescent sections were consecutively viewed at low magnification (2×) on an Olympus® BX61 automated light microscope and captured by an Olympus® CC12 digital video camera mounted on top. (The use of tranverse sections were only used in this imaging as the whole brain could be sectioned with fewer number of histological sections.) The brain sections were too large to be captured within a single field of view. Therefore, each image was assembled from a montage of up to twelve smaller captured regions of interest using Microsuite-B3SV software (Soft Imaging System, Lakewood, CO) controlling a Ludl® motorized stage. The exposure rate was fixed to maintain uniform excitation of the fluorescent-labeled sections with a rhodamine filter cube.

Registration of the dataset. Automatic registration was achieved by choosing control (fiducial) points between adjacent pairs and carrying out a transformation on one image so that it closely matched the other. This was conducted based on correlating two adjacent images at a time—specifically, the TARGET image was registered to the BASE image. For example, when image *i* was registered to *i-1*, the transformation applied to image *i* involved the overall transformation that has been applied to image *i-1* plus the new transformation between images *i* and *i-1*, and so on. In this way, all subsequent images in the data set were finally registered to the first image.

Images were also converted from RGB (red, green, and blue components) to the format of HSV (hue, saturation, and value), and only the value component (intensity) was be used in the later steps. Since our goal was to obtain the corresponding points in the BASE and TARGET images, the most representative corresponding points would be those that critically defined the shape of these features, which were finally defined by the aid of a edge–detection algorithm.

Three-dimensional reconstruction. To ensure accuracy of the three-dimensional (3D) reconstructions, every histological section comprising one data set for each brain was used, except the rare occasion where a histological section was lost or unusable.

In the figure shown, visualizations of injured and uninjured brains were constructed from 246 and 237 serial sections, respectively (Fig. 3). The final 3D reconstruction was accomplished using an isocontouring software application developed by Bajaj et al. (1997) running on a Silicon Graphics® Indigo workstation (Mountain View, CA). This procedure allowed only biological features that were consistent in two or more sections to be 3D reconstructed, thus eliminating any outlier histological defects from the 3D image (Duerstock et al., 2000). The quantification of imbedded structures within the 3D image used a spectral interface to select the isocontours of the whole brain and EB-labeled regions. The wireframe surfaces were automatically divided into tetrahedral subcomponents that were computed using a B-spline function to calculate volume and surface area. These procedures have been standardized, validated, reported, and used in prior investigations (Bajaj et al., 1997; Duerstock et al., 2000, 2003).

Confirmation of Dye Exclusion Test with Horseradish Peroxidase

Given greater experience using horseradish peroxidase (HRP) as an intracellular label in injured nervous tissue (Borgens et al., 1986), we initially confirmed the dye-exclusion test in brain using this label. HRP (40,000 Daltons 30% by volume in 150 μL of saline) was injected two hours after injury or sham injury. These animals were a separate group from those tested with EB, and were sacrificed 8 hours after injection by perfusion with lactated ringers followed by 6% paraformaldehyde 0.5% glutaraldehyde in PBS. Frozen sections were taken as described above. The HRP stained sections were placed in PBS for 10 min. Afterwards, they were immersed in cacodylate buffer (pH 5.1) for 15 min. They were then placed in 0.03% 3,3-diaminobenzadine (DAB) in cacodylate buffer (pH 5.1) for 30 min. Hydrogen peroxide was added to this solution at 0.08% and the sections were allowed to sit another 10 min. Afterwards, they were rinsed in PBS, dehydrated through levels of alcohols as described above, placed in xylene, cover-slipped with permount, and analyzed with the light microscope.

Confirmation of PEG Distribution in Injured Brain

To determine whether PEG could enter regions of interest in damaged brain after intravenous injection, we injected fluorescently-labeled PEG (fluorescein-5-thioureidyl-poly [ethylene glycol] methyl ether [FITC-PEG, Molecular Probes, Eugene, OR], 2500 MW, 1 cc, 30% by volume in saline) into the rat tail vein immediately after injury. Animals were sacrificed 24 h after injury, and the brains were sectioned and prepared as described above. Observations of these sections were made with an Olympus Van Ox Universal fluorescent microscope (excitation filter, BP 495 nm; barrier filter, 0–515 nm; Olympus America Inc., Melville, NY).

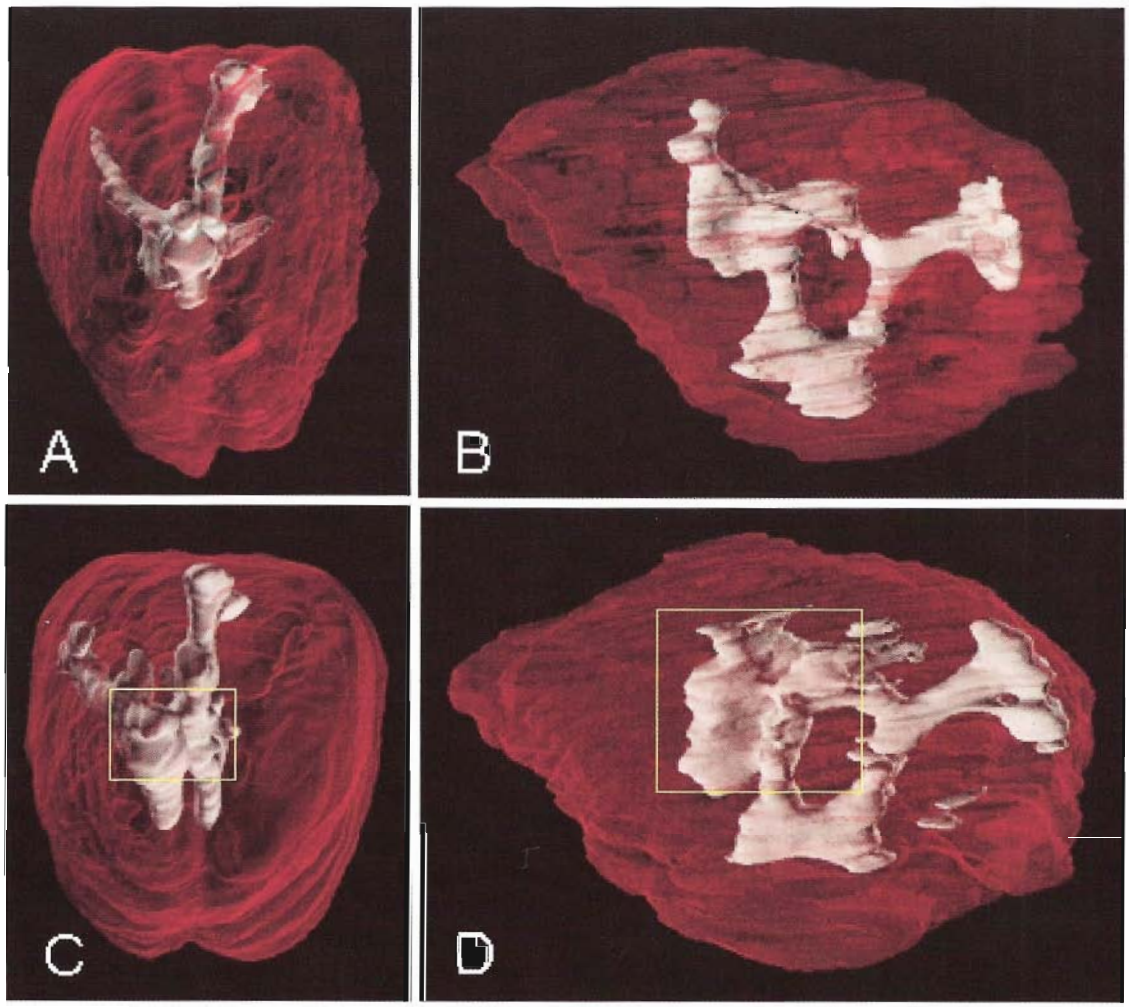

FIG. 3. Ethidium bromide (EB) presence in injured and uninjured brains by three-dimensional reconstructions. A and B show different views of an EB-labeled uninjured rat brain three-dimensionally reconstructed from serial transverse. The brain (rendered in red) was made transparent to reveal the internal region of fluorescence shown in light gray. (**A**) The dorsal surface of the brain (red) is shown with the rostral end toward the bottom of the page. (**B**) Side view of this brain and EB-specific labeling. The frontal lobe is on the right side, dorsal to the top of the page. C and D are separate views of a three-dimensional reconstruction of an injured brain labeled with EB. (C,D) Images are presented in an identical orientation as A and B, respectively. Note that the larger region of fluorescence was associated with injury (yellow box).

RESULTS

Standardization of the Injury Model

The use of this injury model has been reported in various publications (Heath and Vink, 1996; Povlishock et al., 1997; Cernak et al., 2002); however, one parameter was found to be crucial to the standardization of the injury between animals that required further investigation and evaluation. Curiously, this factor was the character of the foam bedding supporting the animal during impact. Calculations of the expected weight rebound were made using data from Marmarou et al., 1994 and compared to physical measurements of the weight rebound onto newly purchased and stored foam (with appreciation of the standard HIC) (Versace, 1971; Margulies and Thibault, 1992). The spring and damping constants (k and μ) measured from bedding foam when new were similar to the parameters reported by Marmarou et al. (1994) (Fig. 4, Table 1). The spring and damping constants for foam aged more than six months and exposed to light were different (k = 2400 and 1200 Nt/m, respectfully; μ = 29 and 25 N-sec/m, respectively). Based on these measurements, we determined that foam must be placed in darkness and discarded after one month of use.

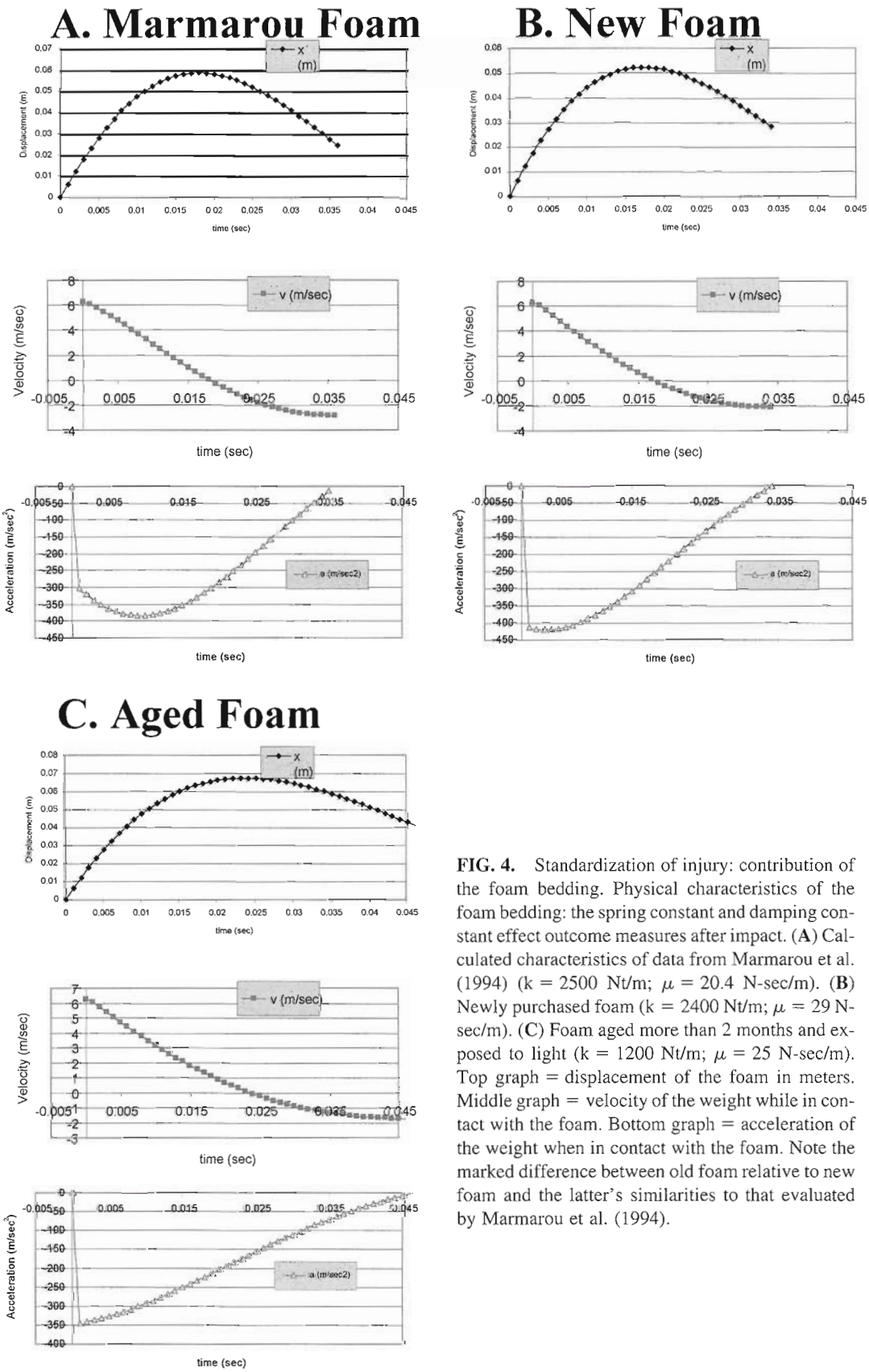

FIG. 4. Standardization of injury: contribution of the foam bedding. Physical characteristics of the foam bedding: the spring constant and damping constant effect outcome measures after impact. (**A**) Calculated characteristics of data from Marmarou et al. (1994) (k = 2500 Nt/m; μ = 20.4 N-sec/m). (**B**) Newly purchased foam (k = 2400 Nt/m; μ = 29 N-sec/m). (**C**) Foam aged more than 2 months and exposed to light (k = 1200 Nt/m; μ = 25 N-sec/m). Top graph = displacement of the foam in meters. Middle graph = velocity of the weight while in contact with the foam. Bottom graph = acceleration of the weight when in contact with the foam. Note the marked difference between old foam relative to new foam and the latter's similarities to that evaluated by Marmarou et al. (1994).

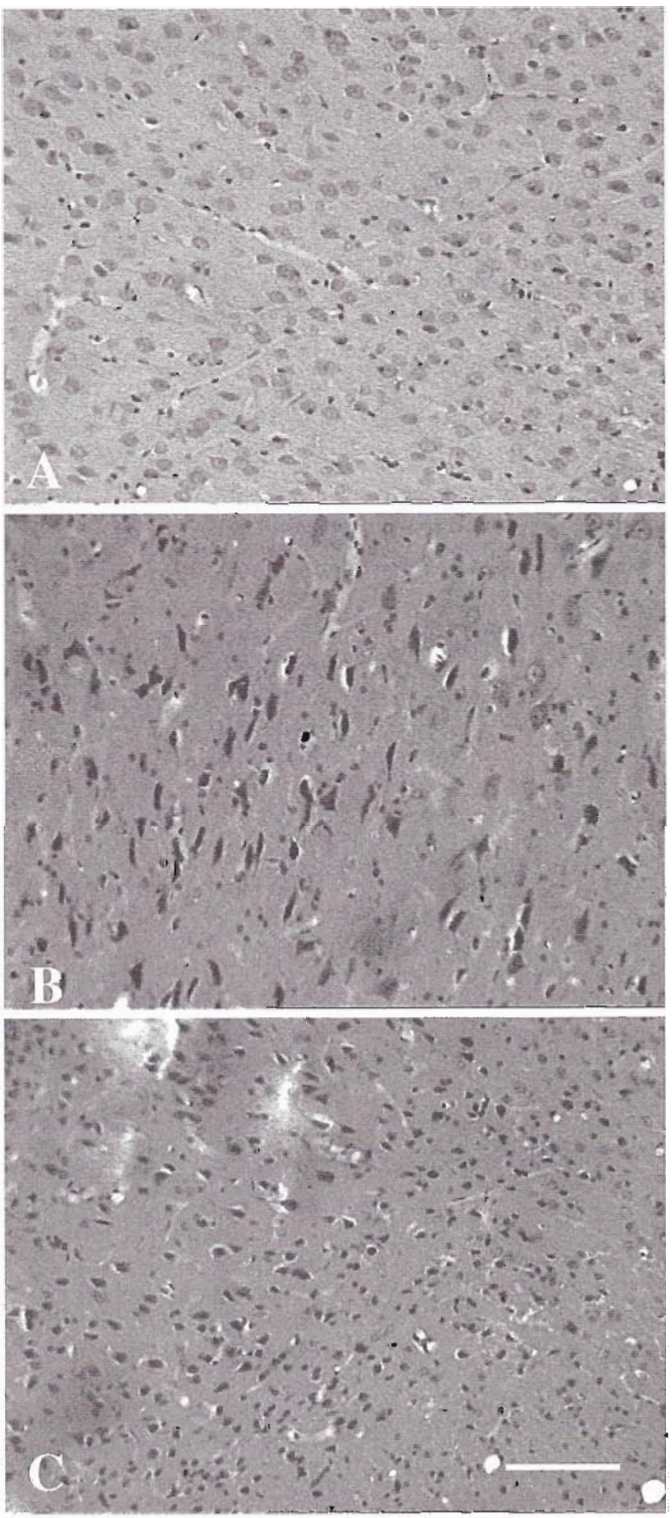

FIG. 5. Qualitative features of impact injury. (**A**) An area of the superficial sensory cortex is shown in an uninjured brain. Note the clear open nuclei with chromatin granules characteristic of uninjured rat brain cortex. (**B**) A similar location in the cortex 24 h after a 1.5-m impact is shown. Note the presence of condensed pyknotic cells. (**C**) Severe injury to the cortex was produced by a 2-m impact. Any evidence for spared neurons in these sections was scant. All brains were stained with Hemotoxylin and Eosin at 24 h after injury or sham treatment. Bar = 100 μm (in C, for all photomicrographs).

Qualitative analysis to confirm a standardized injury to the brain was obtained from the cortex below the impact site using histological sections stained with a standard Harris' Hemotoxylin and conventional histological procedures (Fig. 5). Cortical neurons in rats receiving a severe injury (2-m drop) or moderate injury (1.5 m) illustrated pyknotic characteristics compared to neurons in uninjured control animals and in uninjured regions of the test brains. All further experiments were carried out using the more severe injury (2-m drop).

PEG Enters Damaged Regions of the Brain

Fluorescently labeled PEG crossed the damaged blood–brain barrier after TBI (Fig. 6). We found that fluorescent PEG had entered areas of the injured cortex (Fig. 6A′) but only modestly above the level of detection. There was less fluorescence in uninjured brains in animals injected with fluorescent PEG (Fig. 6B) as compared to uninjured animals that had not been not injected with fluorescent PEG (Fig. 6A). Regions of the brain stem in injured brains receiving fluorescent PEG injection were markedly labeled (Fig. 6B′). The corpus callosum apical to the hippocampus and adjacent to the ventricles was labeled with fluorescent PEG, indicating that the polymer penetrated and diffused throughout this area (Fig. 6C). The accompanying pseudocolor graphic reveals the intense PEG fluorescence associated with the lateral edges of the caudal pontine region after injury, grading to low levels medial to this region (Fig. 6D). In summary, PEG labeling was consistently found in characteristic areas of brain injury experienced in the impact acceleration injury model.

Confirmation of Dye Exclusion Procedures

The procedure of dye exclusion as an index of cellular injury in the central nervous system has been previously established with horseradish peroxidase (HRP) in the spinal cord (Shi and Pryor, 2000) and brain (Singleton and Povlishock, 2004). We qualitatively tested the

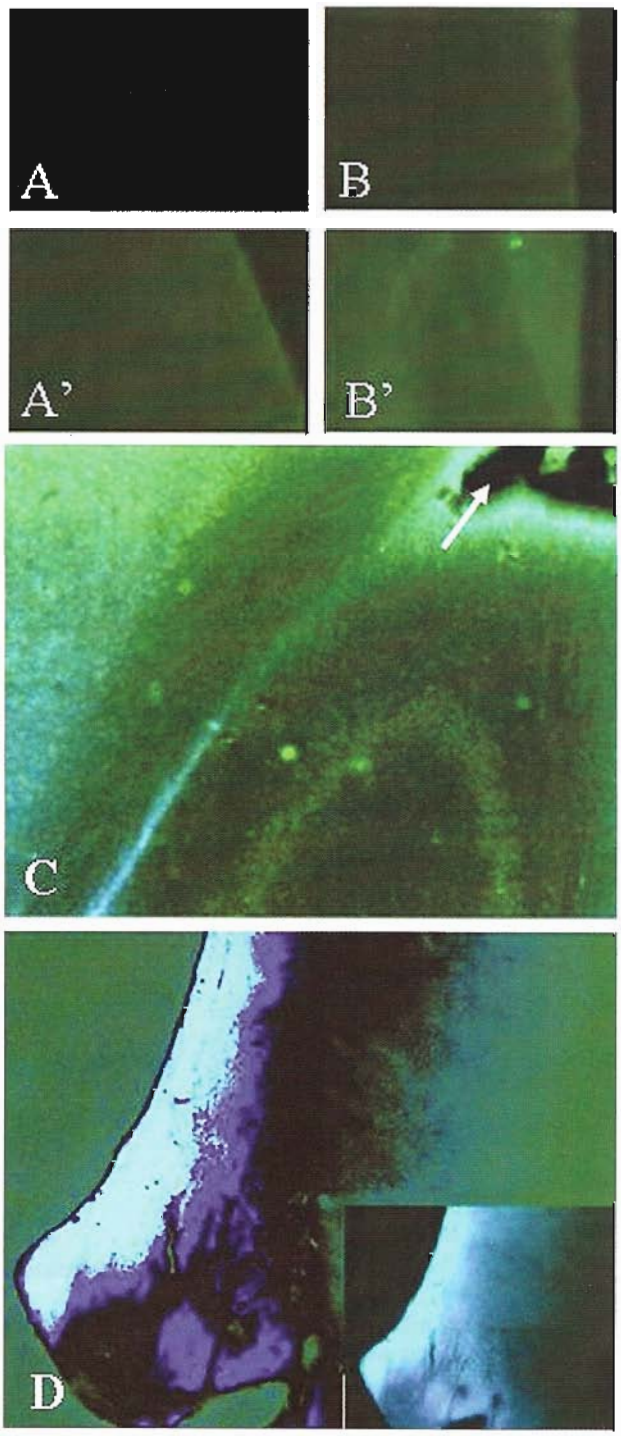

FIG. 6. Polyethylene glycol (PEG) distribution in injured and uninjured brain. Intravenous PEG preferentially labels regions of damage in brain. (**A,B**) In B, intravenously administered fluorescent PEG is barely detectable compared to background fluorescence in regions of uninjured cortex near the saggital fissure; this brain looked similar to the low level of endogenous fluorescence apparent in A, an uninjured brains that did not receive intravenous PEG. (**A′,B′**) In A′, PEG diffusely labeled identical regions of the brain after impact injury; B′ shows the diffuse fluorescence in the brain stem after injury in a rat receiving intravenous PEG injection. These photomicrographs are unaltered video captures. (**C,D**) In C, PEG labeling in a region of the injured corpus callosum (arrow points to the lateral ventricles); D is a pseudocolor image revealing a gradient of PEG labeling from relatively high concentration (light blue), diminishing to dark blue, and black in the lateral edges of the caudal pontine region. (**Inset**) Unaltered video capture of this identical region.

uptake of this more conventional marker secondary to intraventricular injection prior to the routine use of EB. HRP was able to diffuse into the brain to areas such as the cortex dorsal and medial to the cingulum bundle, where damaged cells and portions of cells were clearly marked (Fig. 7A). Cells in an identical region of the control brain showed little to no uptake of HRP compared with the injured brain (Fig. 7B).

Ethidium Bromide

After injection into the left lateral ventricle of the rat brain after injury, EB entered cells near the ventricles, including the axons of the corpus callosum directly apical to the lateral ventricles (Figs. 8B and 9A,B) while EB labeling in uninjured brains was minimal (Figs. 8A and 9C). EB labeling in PEG-treated injured brains was significantly less than that observed in injured brains (Figs. 8C and 9D). Moreover, the minimal level of EB fluorescence in PEG-treated brains was similar to uninjured brains (Table 2).

The fluorescent intensity of EB was first calculated including the lateral and third ventricles (Fig. 10). Injured untreated brains had significantly more fluorescence than both uninjured controls ($p < 0.01$) or injured PEG-

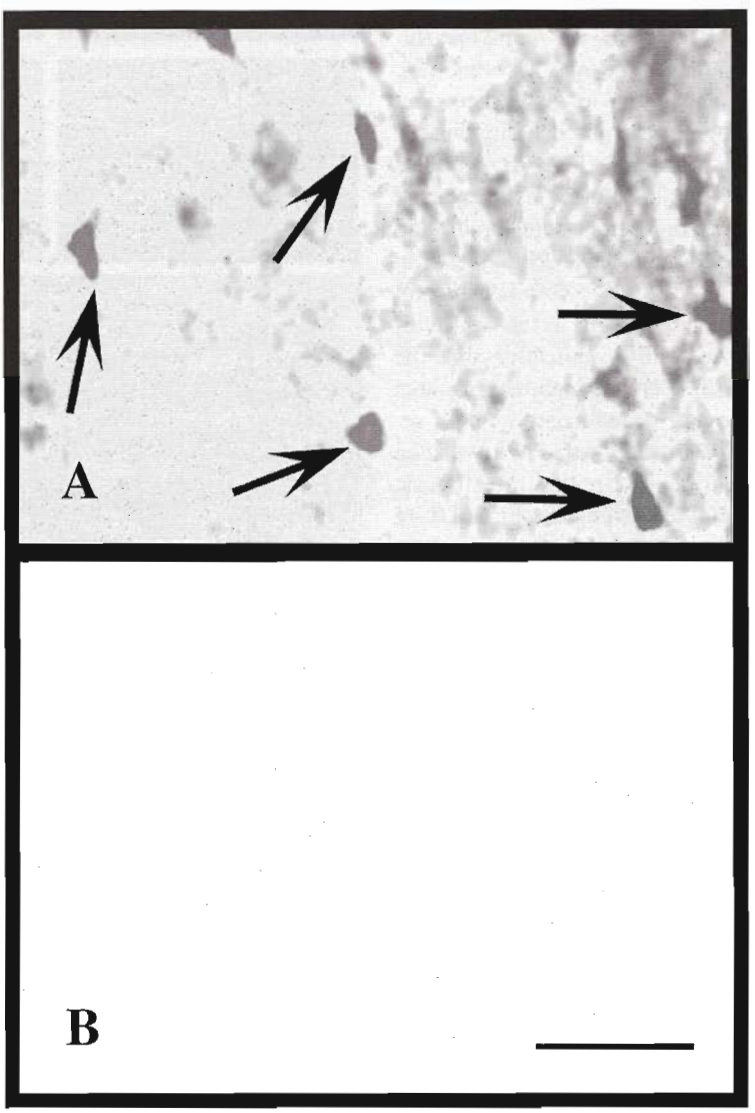

FIG. 7. Dye exclusion procedure. (**A**) Uptake of horseradish peroxidase (HRP; 150 μL, 30% in saline) was injected as shown in Figure 2. Note that the arrows point to well-labeled injured cells that imbibed the marker dorsal and medial to the cingulum bundle. Labeling occurs in cell bodies as well as cell processes such as dendrite and axons. (**B**) Identical regions of an uninjured rat brain treated similarly to the animal shown in A. Note the complete absence of HRP uptake by these cells. Bar = 30 μm.

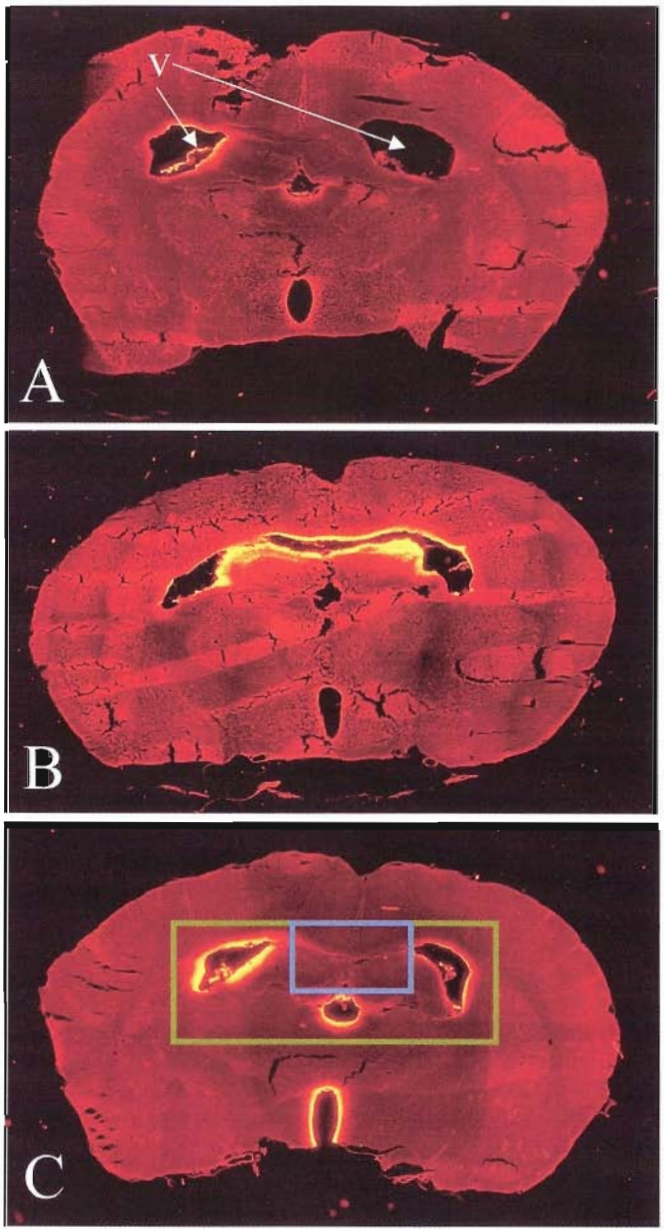

FIG. 8. Ethidium bromide labeling in polyethylene glycol(PEG)–treated and untreated brains. (**A**) Coronal section of an uninjured rat brain is shown caudal to the injection site. Note the fluorescence at the lining of the left ventricle. There is less labeling in this region contralateral to the site of injection. (**B**) Similarly treated but injured rat brain. Note the intense labeling in regions adjacent to, but not limited to, the lining of the ventricle. (**C**) Similar photo montage shows the response to PEG injection in the injured rat brain. Note the more restricted labeling compared to B, and the qualitative similarity to the control brain in A. The green box in C marks the region in which quantitative measures of fluorescence were obtained to include the lateral and third ventricles. The blue box shows the region in which quantitative measures were obtained between the ventricles. Each image is a montage of 16–20 fields of view at original magnification of ×4.

treated brains ($p < 0.01$). The fluorescent intensity in uninjured control and injured PEG-treated brains was also significantly different ($p < 0.05$) when the fluorescence associated with the ventricles was included.

The lining of the ventricles that was labeled in all brains evaluated was excluded in a separate determination of fluorescence (Fig. 11 and Table 3). These measurements clarified EB uptake—limiting evaluation to

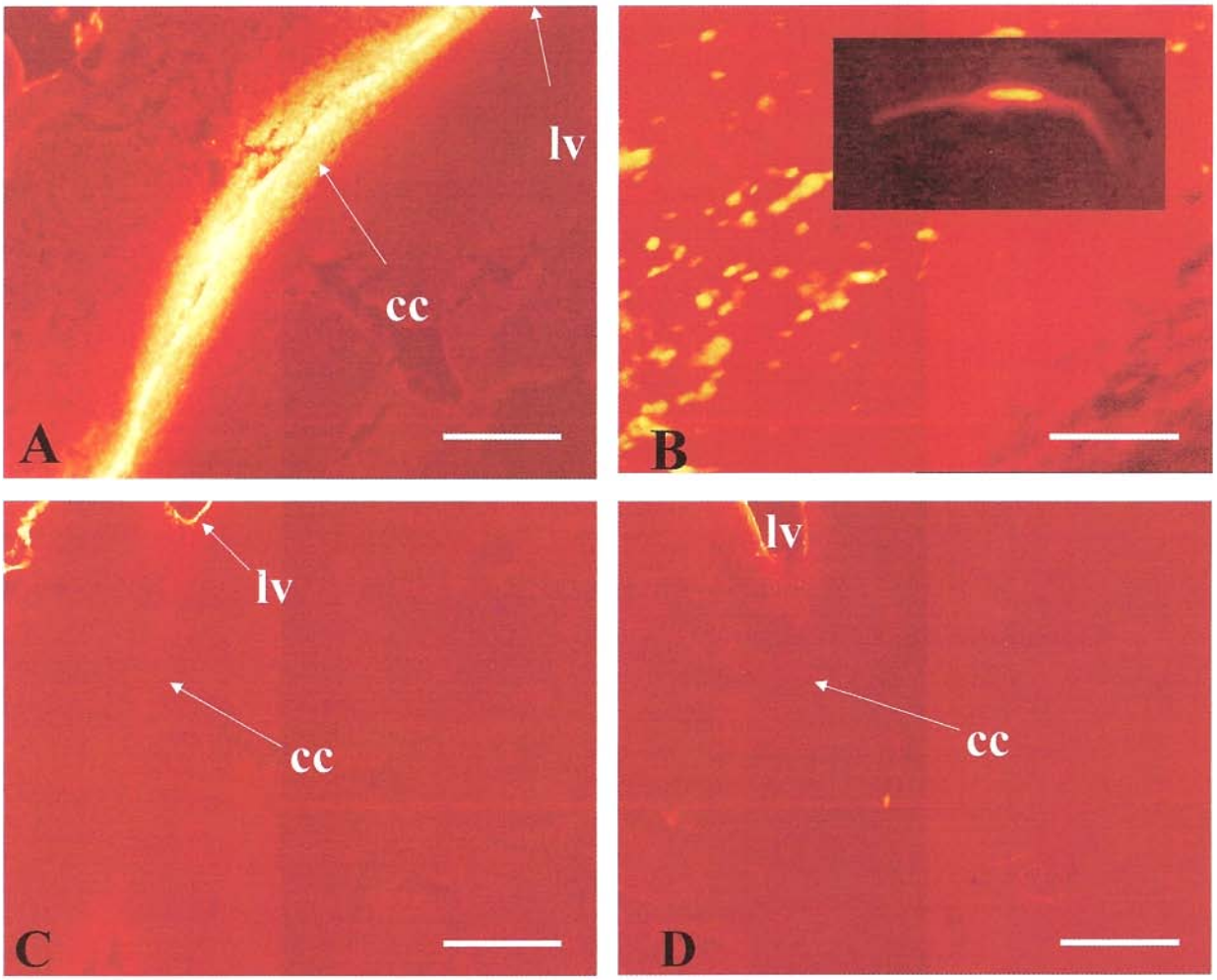

FIG. 9. Rescue of neurons after brain injury in response to intraveneous injection of polyethylene glycol (PEG). (**A**) Region of severe injury of the corpus callosum (cc) after 2-m impact. The intracellular label, as in Figure 8, was ethidium bromide (90 mM in 110 μL of saline). Bar = 0.5 mm. (**B**) Higher magnification view of the same region. Bar = 30 μm. This image reveals that intense fluorescence at low magnification (and in thicker optical section) was due to the aggregate of mainly damaged axons fluorescing after imbibing the marker. Labeling is discontinuous in axons, as ethidium bromide (EB) labels nucleic acids and does not spread uniformly throughout the axoplasm. Other damaged cells, likely oligodendrocytes and other glia (**inset**), were also observed in this region. (**C**) Identical region to A, yet in an uninjured rat brain. Note the presence of fluorescence associated with the epithelium of the lateral ventricle (lv). (**D**) Injured rat brain treated with PEG is shown for comparison. Again, labeling is restricted largely to the epithelial lining of the ventricles. Bar = 0.5 mm (C,D).

deeper regions of the corpus callosum—and the result was essentially the same as described above, yet more marked: PEG-treated and uninjured control animals were not significantly different from each other ($p > 0.05$). Fluorescent intensity in injured yet untreated brains was statistically significantly greater compared to uninjured controls and injured but PEG-treated brains ($p < 0.01$). Fluorescence associated with labeling of only the ventricular lining was normalized ([fluorescent intensity including ventricles] − [fluorescent intensity between ventricles]) which revealed that this labeling was statistically similar between all groups (Fig. 11). Labels that mark cellular inclusions such as EB do not yield the most complete or uniform morphology. Thus, labeling of axons of the corpus callosum was discontinuous. Small cells, likely glia, were also labeled in this region (Fig. 9B). HRP-injected brains provided more familiar morphology of neurons and axons in the region of damage—in particular, the subcortical regions at the unilateral site of impact. Here HRP uptake by cells was heavy in injured animals (but not in the contralateral hemisphere) and absent in uninjured controls (Fig 7). Confirming the data pro-

TABLE 2. QUANTIFICATION OF EB LABELING IN INJURED AND UNINJURED THREE-DIMENSIONAL RECONSTRUCTIONS OF BRAIN

	Brain		*EB labeling*		*Normalization of volume*
	Surface area in mm^2	*Volume in mm^3*	*Surface area in mm^2*	*Volume in mm^3*	*Percentage of labeling in the brain*
Uninjured	755.9	849.1	140.1	36.5	4.3
Injured	958.8	1022.5	218.7	59.4	5.8

The brain reconstructions were quantitatively compared for volume and surface area of the whole brain and the EB-labeled region "embedded" within. The uninjured brain was slightly smaller than the injured subject; therefore, the volume of EB labeling is shown as a percentage of the total brain volume. Though the overall sizes of the brains were different, the sizes of the ventricles were similar. We observed from the reconstructions and the component serial sections that EB labeling consistently revealed the same structures, including the third ventricle and left lateral ventricle. Thus, increased EB labeling in the injured brain constituted greater labeling of parenchyma over that associated with the ventricular spaces. The greatest extent of non-ventricle EB uptake in injured brain occurred rostral and superior to the third ventricle between the cerebral hemispheres. This location was consistent with damage to the corpus callosum. EB, ethidium bromide.

vided by EB, HRP labeling was also vanishingly reduced in PEG-treated, but impacted, brains (Fig. 12 and Table 3).

DISCUSSION

The impact acceleration injury, a closed head injury model, was originally developed to investigate traumatic axonal injury in brain. After standardizing the model and calibrating the foam bedding, we were able to reproduce the characteristics of injury reported previously—including injury to the area of the corpus callosum (Foda et al., 1994). The axons of the corpus callosum show marked uptake of EB in injured brains as EB preferentially diffuses to those cells medial to the ventricles. Less extensive EB migration throughout lesioned regions (compared to HRP) was possibly due to the lesser amount of label used—or because as a smaller molecule it is imbibed rapidly in injured regions near the injection, and is

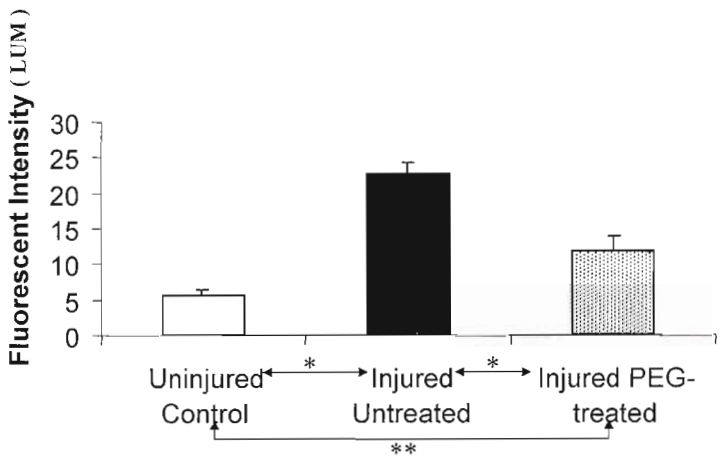

FIG. 10. Quantitative evaluation of fluorescence in experimental rat brains, including ventricles. The means for fluorescent intensity of coronal sections including lateral and third ventricles (green box, Figure 8C). The fluorescent intensity from uninjured controls, injured untreated, and polyethylene glycol (PEG)–treated injured animals ($n = 4$ for each group) were calculated. Note the significant reduction in ethidium bromide fluorescence in injured brains produced by PEG injection ($^*p < 0.01$). The fluorescence associated with ethidium bromide (EB) labeling in PEG-treated brains was significantly reduced compared to injured but untreated brains, yet still elevated relative to uninjured controls ($^{**}p < 0.05$).

unavailable to injured soft tissues at greater distances from the ventricles.

While the ventricular lining may be damaged (and thus labeled) in impacted animals, we do not entirely understand why EB labels uninjured cells of the ventricular lining in uninjured animals. It is not likely that it is aggregating on the "sticky" surfaces of intact cells since complexing with nucleic acids is critical to its fluorescence. It is more likely that the label may be incorporated somehow during the natural turnover of these lining cells and that ependyma may perform some phagocytic functions in brain, thus actively endocytose the marker. When the fluorescence associated with ventricular lining was excluded from consideration however, an even greater difference was observed between injured untreated brains and injured PEG—treated brains. PEG application restricted transmembrane movement of extracellular EB to the inside of damaged cells. Such intracellular labeling was usually intense after TBI. Though our presentation of data has emphasized the tissue level, we emphasize that EB produces negligible fluorescence unless it enters the intracellular compartment and binds

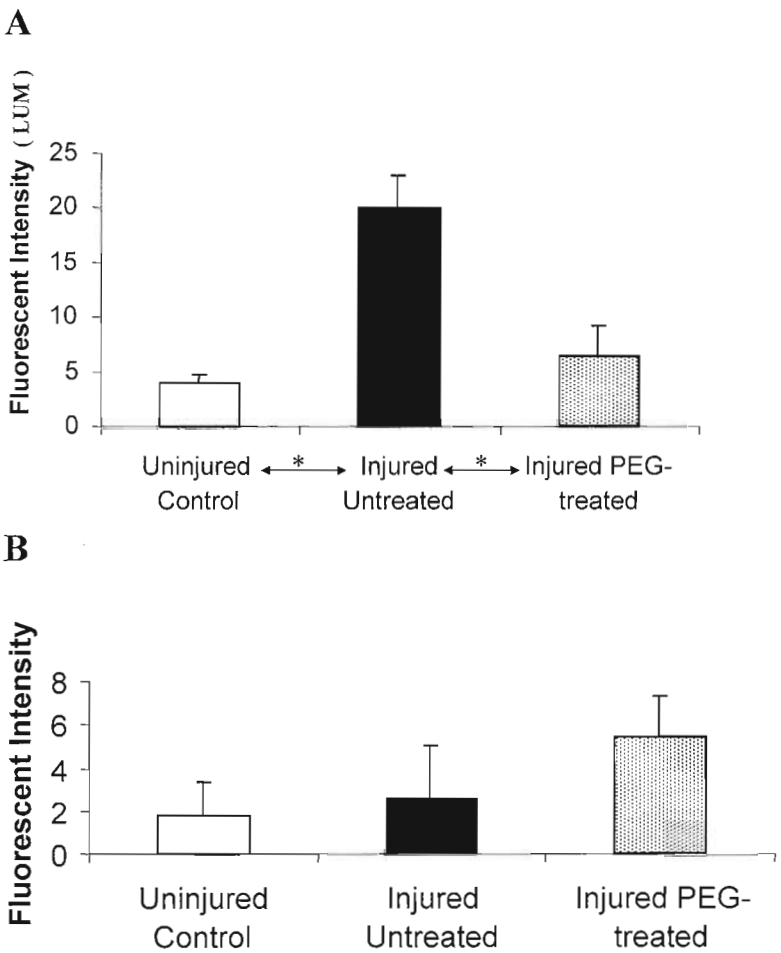

FIG. 11. Quantitative evaluation of fluorescence in experimental rat brains between ventricles. (**A**) Mean fluorescent intensity of coronal sections is shown excluding the superficial labeling of the lateral and third ventricles (blue box, Figure 8C). Ethidium bromide (EB) fluorescence in injured brains produced by polyethylene glycol (PEG) injection differed from injured control brains more dramatically when ventricular fluorescence was not considered ($*p < 0.01$). Statistical significance was similar to that shown in the comparison of uninjured controls and injured untreated animals in Figure 10 ($*p < 0.01$). When the fluorescence associated with the lining cells of the ventricles was not included in evaluations, there was no statistical difference between uninjured controls and injured PEG-treated animals ($**p > 0.05$). (**B**) Means of the difference in fluorescent intensity of coronal sections including (Fig. 10) and excluding (Fig. 11A) ventricles was normalized ([fluorescent intensity including ventricles] − [fluorescent intensity between ventricles]) and compared. There was no significant difference between the groups, indicating that the fluorescence associated with lining cells of the ventricles was statistically similar for all groups.

TABLE 3. FLUORESCENCE DATA IN EXPERIMENTAL RAT BRAINS BETWEEN VENTRICLES

Group	*Total fluorescence*[a]	*Mean*	*Standard error of the mean*	*Range*[b]
Uninjured control	47.00	3.92	0.72	0.46–8.28
Injured untreated	241.39	20.12	2.64	8.70–40.08
Injured PEG-treated	77.79	6.48	2.42	−1.02 to 24.43

[a]Total fluorescence in units of luminosity (LUM) for all histological sections for all animals in this group. For determination of LUM, see text.

[b]A negative value can occur when the background luminosity was higher than the luminosity between the ventricles.

with nucleic acids. Non-neuronal cells, neurons, and axons are replete with such reactive nucleic acids (Sun-Kyung and Hollenbeck, 1995; Koenig and Giuditta, 1999; Piper and Holt, 2004). The intense fluorescence after TBI in (a) regions of the brain vulnerable to impact in this model (such as the CC and superficial cortex), and (b) uninjured controls supports the hypothesis that EB labeling was indicative of significant cell membrane disruption after TBI. This reduction in EB uptake in PEG-treated brains was not associated with some mechanism unrelated to either injury or membrane sealing by PEG since PEG-treated and uninjured control brains were similar. Furthermore, the EB results were consistent with (1) our confirmation of the dye exclusion test using HRP relative to similar observations by others (Singleton and Povlishock, 2004), and the near elimination of this uptake after PEG treatment and (2) the results of similar dye exclusion tests performed using both *in vitro* and *in*

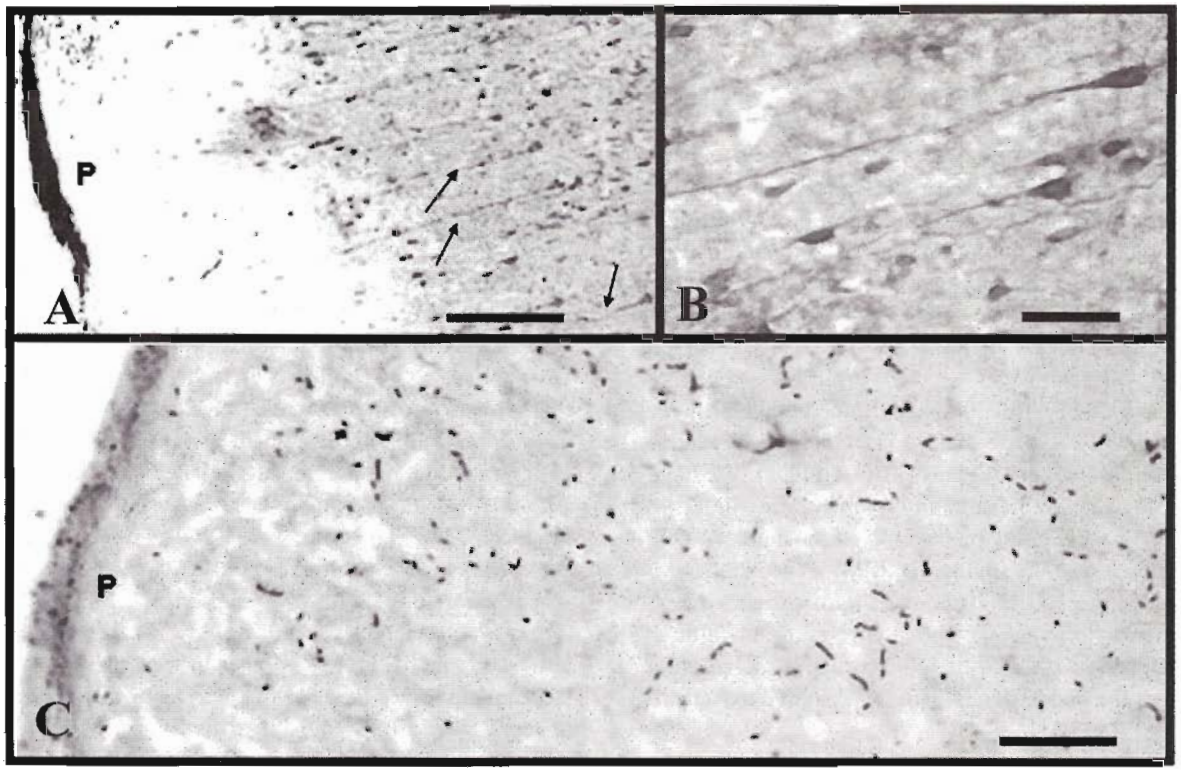

FIG. 12. Horseradish peroxidase (HRP) labeling of subcortical neurons in injured and polyethylene glycol (PEG)–treated brains. (**A**) A low magnification view of the subcortical region of a rat brain beneath the site of impact is shown. Note that damaged neurons are clearly labeled with HRP, including their long axons (arrows). (**B**) A higher magnification view of these cells. (**C**) Montage shows this identical region, but in an injured and PEG-treated animal. Note the complete lack of HRP-labeled CNS cells. Bar = 250 μm (A), 50 μm (B), 100 μm (C).

vivo spinal cord with both labels (Luo et al., 2002; Shi and Pryor, 1999). It could also be that the time course of EB uptake may be affected by PEG; however, this seems less relevant to these results, given that the loss of intracellular labels is also vitiated by PEG.

Molecular Markers as Indices of Membrane Disruption and Sealing

In the reports cited here, we have suggested that it is likely a wide range of membrane defects may be repaired/restored by inorganic polymer administration—and in all damaged cells, including non-neuronal support cells of the CNS (Borgens 2001 and 2003).

Electrical excitability is immediately restored in crushed spinal cord in organ culture following PEG application—though the magnitude of recovered compound action potentials (CAP) are clearly enhanced after a subsequent administration of a fast potassium channel blocker (4-aminopyridine) to the bathing medium (Shi and Borgens, 1999). The most parsimonious interpretation of this result is that the very rapid sealing ability of PEG (seconds to minutes) sufficient to restore CAP initiation and conduction, likely reduced the extent of ionic derangement after mechanical injury (restoring to some degree the permeability barrier to even ions). This seal is incomplete at the level of ion channels however, or potassium blockade would have no effect on the shape or magnitude of restored CAPS in the presence of PEG.

In the injured spinal cord, we have used the loss of Lactate Dehydrogenase (LDH) from the intracellular compartment into the extracellular milieu after injury as an index of cell compromise. PEG application significantly reduced the transmembrane movement of this label (Luo et al., 2002). Thus PEG is able to seal membrane breaches in mammalian CNS cells sufficient to inhibit (a) the loss of very large markers from the cell such as LDH (~160,000 Da), (b) the uptake of modestly large labels (HRP; ~40,000 Da), and (c) the uptake of very small markers such as EB (~400 Da). We have not yet fully explored the nature of membrane breaches repaired by PEG based on the MW of the markers. Our impression is that the smaller the MW of the label, the more intensive the labeling (as one might expect) in injured cord or brain in situ, or spinal cord in organ culture (Shi and Borgens, 2000)—though the overall spread of the label within the tissue is a more complicated and paradoxical issue.

We have not quantitatively established this by comparison however. Rather we have begun investigations to directly observe the imperfections in the living cell membrane using atomic force microscopy (AFM), where the AFM tip can be used to produce a rigorously controlled nano puncture to the membrane—and then backed away from the insult to image it. Already this procedure has been used to image neuron cell death in real time, and the "exsanguination" of cytosol after mechanical injury in living DRG and Sympathetic ganglion cells in vitro. The puncture to living nerve membrane using the AFM cantilever tip was precisely controlled to be 50 nm wide and 400 nm deep and a single puncture or slice killed the cell within 0.5 h. A pool of degraded cytoplasm formed (and progressively increased in size) on the substrate coincident with the collapse of the cell body (McNalley and Borgens, 2003). Our ongoing study is to image polymer-mediated sealing with AFM technique.

Sealing and Fusion of Membranes using Inorganic Polymers

Taken together these investigations suggest a characteristic, but generalized, mechanism of PEG action in reversing or eliminating cell and tissue necrosis after mechanical injury is via a "repair" of the compromised membranes This reconstitution of the membrane enables it to function, once again, as an effective "fence" preventing sufficient co-mingling of the solutes of the intracellular and extracellular compartments and permitting action potential conduction in excitable cells (Shi and Borgens, 1999). These factors act in concert to provide protection in damaged cells from progressive deterioration.

PEG as a Fusogen and Agent of Membrane Repair

As revealed in this study of TBI, and in previous studies of SCI, an injectable, water-soluble PEG possesses a unique ability repair cell membranes. Indeed, transected axons of adult guinea pig white matter can be functionally and anatomically reconnected (i.e., fused). Originally, this capability was first exploited to induce the formation of hybridomas during the production of monoclonal antibodies, as well as facilitating vesicular fusion in model membrane studies (Lee and Lentz, 1997; Ahkong et al., 1987; Davidson et al., 1976; O'Lague and Huttner, 1980; Nakajima and Ikada, 1994). Over 18 years ago, individual giant axons of crayfish and earthworm were fused with PEG following complete transection (Bittner et al., 1986; Krause and Bittner, 1990; Krause et al., 1991). Membrane fusion occurs when adjacent membranes touch in the presence of PEG and this appears to be a prerequisite to the complete fusion of the plasmalemma and the mixing of the cytoplasm of fused cells (Ahkong et al., 1987). It is thought that acute dehydration of the fusing plasmalemmas permits glycol/protein/lipidic structures to resolve into each other at the outer membrane leaflet first and the inner membrane leaflet subsequently (Lee and Lentz, 1997), although the

exact biophysical mechanisms underlying fusion and repair of membranes is still an active area of investigation (Lee and Lentz, 1997; Borgens, 2003). After more than 25 years of investigation of the fusogenic properties of certain polymers and non-ionic surfactants, it is still an incompletely understood area of membrane physics. We hasten to add that the agreed upon mechanisms of cell fusion—which involves the polymer mediation of the structure of membrane water, and the resolution/ intermingling of the lipid phase of the bilayer may not be typical of the repair of minor mechanical defects in membranes. It is likely that "fusion" and "repair" processes may share, and differ, in their mechanisms at the membrane—altogether an area still ripe for investigation.

In any event, organ culture experiments using isolated spinal cord of guinea pigs revealed that a short duration (~2 min) application of PEG could fuse previously severed myelinated axons in completely transected spinal cords sufficient to permit the diffusion of intracellular markers throughout the reconnected segments (Shi et al., 1999). Using similar organ cultured cords, PEG was able to immediately recover conduction of action potentials lost after a standardized crush lesion (Shi and Borgens, 1999). Since the repair of cells secondary to crush or contusion lesions is of more clinical relevance, these data set the stage for testing of topically applied, and intravenous applications of polymers in whole animal neurotrauma studies (Borgens, 2003).

Clinical Implications of Cell Fusion and Repair by Polymers

Topical and intravenous administration of PEG to spinal cord injury models in adult guinea pigs has resulted in significant sparing of white matter, recovery of behavioral functioning, and recovery of conduction through the lesion (Borgens and Shi, 2000; Borgens and Bohnert, 2001; Borgens et al., 2002). We have traced the distribution of fluorescently decorated PEG in spinal cord injured animals after intravenous, intraperitoneal, subcutaneous, and topical applications. We were unable to suggest that any one means of administration was better than another at labeling lesioned areas of the spinal cord (Borgens and Bohnert, 2001). This further suggests that once the polymer gains access to the vasculature, it targets regions of soft tissue damage, but does not accumulate or linger in undamaged tissues since fluorescent PEG is not observed in various control applications (Borgens and Bohnert, 2001; Borgens, 2003). In crushed peripheral nerve, it was required to inject PEG beneath the perineural sheath near the lesion to affect physiological and functional recovery in a sciatic/gastrocnemius muscle injury model (Donaldson et al., 2002). Thus, it appears that administration of this agent is not problematic, and given the strong safety record of PEG administration in human medicine (Working et al., 1997) suggests clinical possibilities for the use of this and other surfactants as potential therapies for clinical neurotrauma. Recently, encouraging results were seen with both intravenous PEG and Poloxamer 188 injection in dogs with severe (neurologically complete) naturally occurring paraplegia (Laverty et al, 2004). Significant and rapid recovery of several outcome measures in dogs, including: deep and superficial pain, ambulation, proprioception, and evoked potentials, was consistent with the functional recovery data reported in spinal injured guinea pigs. We now believe PEG may likely be significant to the treatment of traumatic brain injury as well.

Further Studies

The movement of intravenously applied PEG across both the damaged and (likely) intact blood–brain barrier remains to be better understood. In damaged brains—the movement of decorated PEG into the CNS compartment as shown here for brain and in spinal cord is clear (Borgens and Bohnert, 2001). In other experiments, PEG application was delayed for 8–12 h after injury and still facilitated sealing. Polymer administration (PEG and Poloxamer 188) to clinical cases of paraplegia produced behavioral recovery even when the intravenous injections were made ~72 h post-injury—a time when the BBB would been expected to again be intact. PEG may even play a role in sealing this barrier between the CNS and PNS. We have preliminary evidence that PEG indeed can seal endothelium. A drying of the wounds during laminectomy procedures (by reducing capillary seepage) was routinely observed, but not reported, when PEG was applied directly to the spinal cord and surrounding tissues in guinea pig and clinical cases of paraplegia in dog (Borgens and Shi, 2000; Laverty et al., 2004). This consistent observation prompted the investigation of endothelial sealing by polymers. These data, further details of the movement of PEG after the BBB has spontaneously repaired, chronic TBI, and a more detailed evaluation of cell death and polymer "rescue" *in situ* through the use of a marker for degenerating end bulbs of axons (β–amyloid precursor protein) are studies now completed. These will be reported elsewhere.

ACKNOWLEDGMENTS

We thank Dr. Jian Luo and Deborah Bohnert for their expert assistance in technical matters, Stacey Foyler for manuscript preparation, and Kimberly Harrington for the illustrations. We acknowledge financial support from the

State of Indiana and Mari Hulman George. Financial support was also provided by Purdue University Neuroscience GAANN Fellowship (to A.O.K.), National Science Foundation (HRD-022-7992 to B.D. and R.B.B.) and the support of the CPR by Intel Corporation for the generous gifts of computer equipment. We acknowledge the expert assistance of Dr. John Povlishock and his laboratory, in particular Richard Singleton, for their time spent and valuable help during the early stages of this investigation.

REFERENCES

AESCHBACHER, M., REINHARDT, C.A., and ZBINDEN, G. (1986). A rapid cell membrane permeability test using fluorescent dyes and flow cytometry. Cell Biol. Toxicol. **2,** 247–255.

AHKONG, Q.F., DESMAZES, J.P., GEORGESCAULD, D., et al. (1987). Movements of fluorescent probes in the mechanism of cell fusion induced by poly(ethylene glycol). J. Cell Sci. **88,** 389–398.

BAJAJ, C.L., PASCUCCI, V., and SCHIKORE, D.R. (1997). The contour spectrum. Proceedings of the 1997 IEEE Visualization Conference, 167–173, Oct. 1997, Phoenix, AZ.

BITTNER, G.D., BALLINGER, M.L., and RAYMOND, M.A. (1986). Reconnection of severed nerve axons with polyethylene glycol. Brain Res. **367,** 351–355.

BORGENS, R.B. (1988). Voltage gradients and ionic currents in injured and regenerating axons. Adv. Neurol. **47,** 51–66.

BORGENS, R.B. (2001). Cellular engineering: molecular repair of membranes to rescue cells of the damaged nervous system. Neurosurgery **49,** 370–379.

BORGENS, R.B. (2003). Restoring function to the injured human spinal cord, in: Adv Anat Embryol Cell Biology. P. Beck, B. Christ, W. Kriz, et al. (eds), Springer: Heidelberg, pps. III–IV,1–155.

BORGENS, R.B., and SHI, R. (2000). Immediate recovery from spinal cord injury through molecular repair of nerve membranes with polyethylene glycol. FASEB **14,** 27–35.

BORGENS, R.B., and BOHNERT, D. (2001). Rapid recovery from spinal cord injury following subcutaneously administered polyethylene glycol. J. Neurosci. Res. **66,** 1179–1186.

BORGENS, R.B., BLIGHT, A.R., and MURPHY, D.J. (1986). Axonal regeneration in spinal cord injury: a perspective and new technique. J. Comp. Neurol. **250,** 157–167.

BORGENS, R.B., SHI, R., and BOHNERT, D. (2002). Behavioral recovery from spinal cord injury following delayed application of polyethylene glycol. J. Exp. Biol. **205,** 1–12.

BUKI, A., FARKAS, O., DOCZI, T., et al. (2003). Preinjury administration of the calpain inhibitor mdl-28170 attenuates traumatically induced axonal injury. J. Neurotrauma **20,** 261–268.

CERNAK, I., CHAPMAN, S.M., HAMLIN, G.P., et al. (2002). Temporal characterisation of pro- and anti-apoptotic mechanisms following diffuse traumatic brain injury in rats. J. Clin. Neurosci. **9,** 565–572.

DAVIDSON, R.L., O'MALLEY, K.A., and WHEELER, T.B. (1976). Induction of mammalian somatic cell hybridization by polyethylene glycol. Somat. Cell Genet. **2,** 271–280.

DEY, C.S., and MAJUMDER, G.C. (1988). A simple quantitative method of estimation of cell-intactness based on ethidium bromide fluorescence. Biochem. Int. **17,** 367–374.

DONALDSON, J., SHI, R., and BORGENS, R. (2002). Polyethylene glycol rapidly restores physiological functions in damaged sciatic nerves of guinea pigs. Neurosurgery **50,** 147–156.

DUERSTOCK, B.S., BAJAJ, C.L., PASCUCCI, V., et al. (2000). Advances in three-dimensional reconstruction of the experimental spinal cord injury. Comput. Med. Imaging Graph. **24,** 389–406.

DUERSTOCK, B.S., BAJAJ, C.L., and BORGENS, R.B. (2003). A comparative study of the quantitative accuracy of three-dimensional reconstructions of spinal cord from serial histological sections. J. Microsc. **210,** 138–148.

FENG, Y., FRATKIN, J.D., and LEBLANC, M.H. (2003). Inhibiting caspase-8 after injury reduces hypoxic-ischemic brain injury in the newborn rat. Eur. J. Pharmacol. **481,** 169–173.

FODA, M.A., and MARMAROU, A. (1994). A new model of diffuse brain injury in rats. Part ii: Morphological characterization. J. Neurosurg. **80,** 301–313.

GWAG, B.J., CANZONIERO, L.M., SENSI, S.L., et al. (1999). Calcium ionophores can induce either apoptosis or necrosis in cultured cortical neurons. Neuroscience. **90,** 1339–1348.

HEATH, D.L., and VINK, R. (1996). Traumatic brain axonal injury produces sustained decline in intracellular free magnesium concentration. Brain Res. **738,** 150–153.

KEANE, R.W., KRAYDIEH, S., LOTOCKI, G., et al. (2001). Apoptotic and anti-apoptotic mechanisms following spinal cord injury. J. Neuropathol. Exp. Neurol. **60,** 422–429.

KOENIG, E., and GIUDITTA, A., (1999). Protein-synthesizing machinery in the axon compartment. Neuroscience **89,** 5–15.

KOIZUMI, H., and POVLISHOCK, J.T (1998). Posttraumatic hypothermia in the treatment of axonal damage in an animal model of traumatic axonal injury. J. Neurosurg. **89,** 303–309.

KRAUSE, T.L., and BITTNER, G.D. (1990). Rapid morphological fusion of severed myelinated axons by polyethylene glycol. Proc. Natl. Acad. Sci. USA **87,** 1471–1475.

KRAUSE, T.L., MARQUIS, R.E., LYCKMAN, A.W., et al. (1991). Rapid artificial restoration of electrical continuity across a crush lesion of a giant axon. Brain Res. **561,** 350–353.

LAVERTY, P.H., LESKOVAR, A., BREUR, G.J., et al. (2004). A preliminary study of intravenous surfactants in paraplegic

dogs: polymer therapy in canine clinical SCI. J. Neurotrauma **21,** 1767–1777.

LEE, J., and LENTZ, B.R. (1997). Evolution of lipidic structures during model membrane fusion and the relation of this process to cell membrane fusion. Biochemistry **36,** 6251–6259.

LUO, J., BORGENS, R.B., and SHI, R. (2002). Polyethylene glycol immediately repairs neuronal membranes and inhibits free radical production after acute spinal cord injury. J. Neurochem. **83,** 471–480.

LUO, J., BORGENS, R., and SHI, R. (2004). Polyethylene glycol improves function and reduces oxidative stress in synaptosomal preparations following spinal cord injury. J. Neurotrauma **21,** 994–1007.

MARGULIES, S.S., and THIBAULT, L.E. (1992). A proposed tolerance criterion for diffuse axonal injury in man. J. Biomech. **25,** 917–923.

MARMAROU, A., FODA, M.A., VAN DEN BRINK, W., et al. (1994). A new model of diffuse brain injury in rats. Part 1: Pathophysiology and biomechanics. J. Neurosurg. **80,** 291–300.

McNALLY, H.A., and BORGENS, R.B. (2004). Three-dimensional imagining of living and dying neurons with atomic force microscopy. J. Neurocytol. **33,** 251–258.

MOVSESYAN, V.A., YAKOVLEV, A.G., FAN, L., et al. (2001). Effect of serine protease inhibitors on posttraumatic brain injury and neuronal apoptosis. Exp. Neurol. **167,** 366–375.

NAKAJIMA, N., and IKADA, Y. (1994). Fusogenic activity of various water-soluble polymers. J. Biomater. Sci. Polymer Ed. **6,** 751–759.

NAWASHIRO, H., SHIMA, K., and CHIGASAKI, H. (1995). Immediate cerebrovascular responses to closed head injury in the rat. J. Neurotrauma **12,** 189–197.

O'LAGUE, P.H., and HUTTNER, S.L. (1980). Physiological and morphological studies of rat pheochromocytoma cells (pc12) chemically fused and grown in culture. Proc. Natl. Acad. Sci. USA **77,** 1701–1705.

PIPER, M., and HOLT, C. (2004). RNA translation in axons. Annu. Rev. Cell. Dev. Biol. **20,** 505–523.

POVLISHOCK, J.T., MARMAROU, A., McINTOSH, T., et al. (1997). Impact acceleration injury in the rat: evidence for focal axolemmal change and related neurofilament sidearm alteration. J. Neuropathol. Exp. Neurol. **56,** 347–359.

RAGHUPATHI, R., GRAHAM, D.I., and McINTOSH, T.K. (2000). Apoptosis after traumatic brain injury. J. Neurotrauma **17,** 927–938.

ROY, M., and SAPOLSKY, R. (1999). Neuronal apoptosis in acute necrotic insults: why is this subject such a mess? Trends Neurosci. **22,** 419–422.

SHAPIRA, Y., YADID, G., COTEV, S., et al. (1989). Accumulation of calcium in the brain following head trauma. Neurol. Res. **11,** 169–172.

SHI, R., and BORGENS, R.B. (1999). Acute repair of crushed guinea pig spinal cord by polyethylene glycol. J. Neurophysiol. **81,** 2406–2414.

SHI, R., and PRYOR, J.D. (2000). Temperature dependence of membrane sealing following transection in mammalian spinal cord axons. Neuroscience **98,** 157–166.

SHI, R., and BORGENS, R.B. (2000). Anatomical repair of nerve membranes in crushed mammalian spinal cord with polyethylene glycol. J. Neurocytol. **29,** 633–643.

SHI, R., BORGENS, R.B., and BLIGHT, A.R. (1999). Functional reconnection of severed mammalian spinal cord axons with polyethylene glycol. J. Neurotrauma **16,** 727–738.

SINGLETON, R.H., and POVLISHOCK, J.T. (2004). Identification and characterization of heterogeneous neuronal injury and death in regions of diffuse brain injury: evidence for multiple independent injury phenotypes. J. Neurosci. **24,** 3543–3553.

SUN-KYUNG, L., and HOLLENBECK, P.J. (1995). Organization and translation of mRNA in sympathetic axons. J. Cell Sci. **116,** 4467–4478.

TENG, Y.D., CHOI, H., ONARIO, R.C., et al. (2004). Minocycline inhibits contusion-triggered mitochondrial cytochrome c release and mitigates functional deficits after spinal cord injury. Proc. Natl. Acad. Sci. USA **101,** 3071–3076.

THURMAN, D.J., ALVERSON, C., DUNN, K.P., et al. (1999). Traumatic brain injury in the United States: a public health perspective. J. Head Trauma Rehabil. **14,** 602–615.

VERSACE, J. (1971). *A Review of the Severity Index.* Society of Automotive Engineers: New York.

VINK, R., NIMMO, A.J., and CERNAK, I. (2001). An overview of new and novel pharmacotherapies for use in traumatic brain injury. Clin. Exp. Pharmacol. Physiol. **28,** 919–921.

WORKING, P., NEWMAN, M., JOHNSON, J., et al. (1997). Safety of poly(ethyleneglycol) and poly(ethyleneglycol) derivatives, in: *Poly(ethyleneglycol) Chemistry and Biological Applications.* J.M. Harris and S. Zalipsky (eds), American Chemistry Society: Washington, DC., pps. 45–57.

ZIPFEL, G.J., BABCOCK, D.J., et al. (2000). Neuronal apoptosis after CNS injury: the roles of glutamate and calcium. J. Neurotrauma **17,** 857–869.

Address reprint requests to:
Richard B. Borgens, Ph.D.
Center for Paralysis Research
Purdue University
408 S. University St.
West Lafayette, IN 47907-2096

E-mail: cpr@purdue.edu